JACS
JOURNAL OF THE AMERICAN CHEMICAL SOCIETY
pubs.acs.org/JACS

Article

Light-Mediated Interconversion between a Foldamer and a Self-Replicator

Yulong Jin,* Pradeep K. Mandal, Juntian Wu, Armin Kiani, Rui Zhao, Ivan Huc,* and Sijbren Otto*

Cite This: J. Am. Chem. Soc. 2024, 146, 33395−33402

Read Online

ACCESS | Metrics & More | Article Recommendations | Supporting Information

ABSTRACT: Self-replicating molecules and well-defined folded macromolecules are of great significance in the emergence and evolution of life. How they may interconnect and affect each other remains largely elusive. Here, we demonstrate an abiotic system where a single building block can oligomerize to yield either a self-replicating molecule or a foldamer. Specifically, agitation of a disulfide-based dynamic combinatorial library at moderately elevated pH channels it selectively into a self-replicating hexamer assembled into fibers, after passing through a period where a 15-subunit macrocyclic foldamer existed transiently. Without mechanoagitation or at lower pH, the formation of hexamer fiber is suppressed, resulting in the accumulation of the 15mer foldamer. Foldamer and self-replicator can be interconverted in response to external stimuli, including agitation and a change in pH. Furthermore, upon the addition of a photoacid, the pH of the medium can be controlled by irradiation, driving the switching between replicator and foldamer and allowing a dissipative out-of-equilibrium state to be accessed, using light as a source of energy.

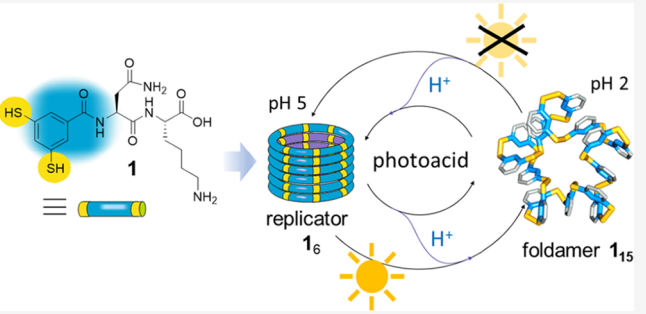

INTRODUCTION

Molecules that can self-replicate or fold are of great significance in the emergence and early evolution of life.[1−3] In nature, replication is done with nucleic acids, while folded molecules like proteins exert other diverse functions, such as molecular recognition and catalysis. Through the central dogma of molecular biology, the information stored in nucleic acids is translated into proteins. However, in primitive life, the complex biochemical machinery that currently mediates transcription and translation was unlikely to be present, raising the question of how folded and self-replicating oligomers can become connected.

Before addressing this question, let us briefly survey the largely unconnected work on synthetic self-replicating molecules and synthetic foldamers. Traditionally, both replicators[1,4−10] and foldamers[11−19] have developed based on rational design, often inspired by their biological counterparts. More recently, it has been shown that both classes of molecules can also emerge spontaneously from dynamic combinatorial libraries (DCLs).[20] In this approach, the noncovalent interactions that form intramolecularly within a specific library member, or intermolecularly between library members, drive the formation of specific foldamers[21,22] or self-replicators,[23,24] respectively, which often have structures that would not be readily accessible by design.

Whether foldamers or self-replicators emerge from dynamic combinatorial libraries is determined by whether noncovalent interactions form intra- or intermolecularly. This means that both compound classes can have a lot in common. In fact, we previously observed that both can form from the same building blocks.[25,26] However, at equilibrium, only one of them (often the self-replicator) will remain. Hence, allowing access to both will require a means of maintaining the system away from equilibrium.

Inspired by nature, chemists are increasingly interested in developing approaches to maintain synthetic chemical systems away from equilibrium, driven by chemical fuels,[27−31] electrically,[32] or through photoirradiation.[33,34]

Here, we demonstrate the autonomous formation of a self-replicator and a foldamer from the same building block as well as the efficient interconversion between them by applying mechanical energy or by a pH change. We also show that upon using a photoacid, photoirradiation can maintain the system away from equilibrium, driving the conversion of the self-replicator to the foldamer. The foldamer only persists as long as irradiation is continued; as soon as it is switched off, the replicator regains dominance.

Received: July 5, 2024
Revised: November 11, 2024
Accepted: November 14, 2024
Published: November 26, 2024

Scheme 1. Oxidation by Air of a Solution of Dipeptide-Appended Dithiol Building Block 1 in Water Yields a Dynamic Combinatorial Library (DCL) from Which Foldamer 1_{15} and Self-Replicator 1_6 Can Emerge[a]

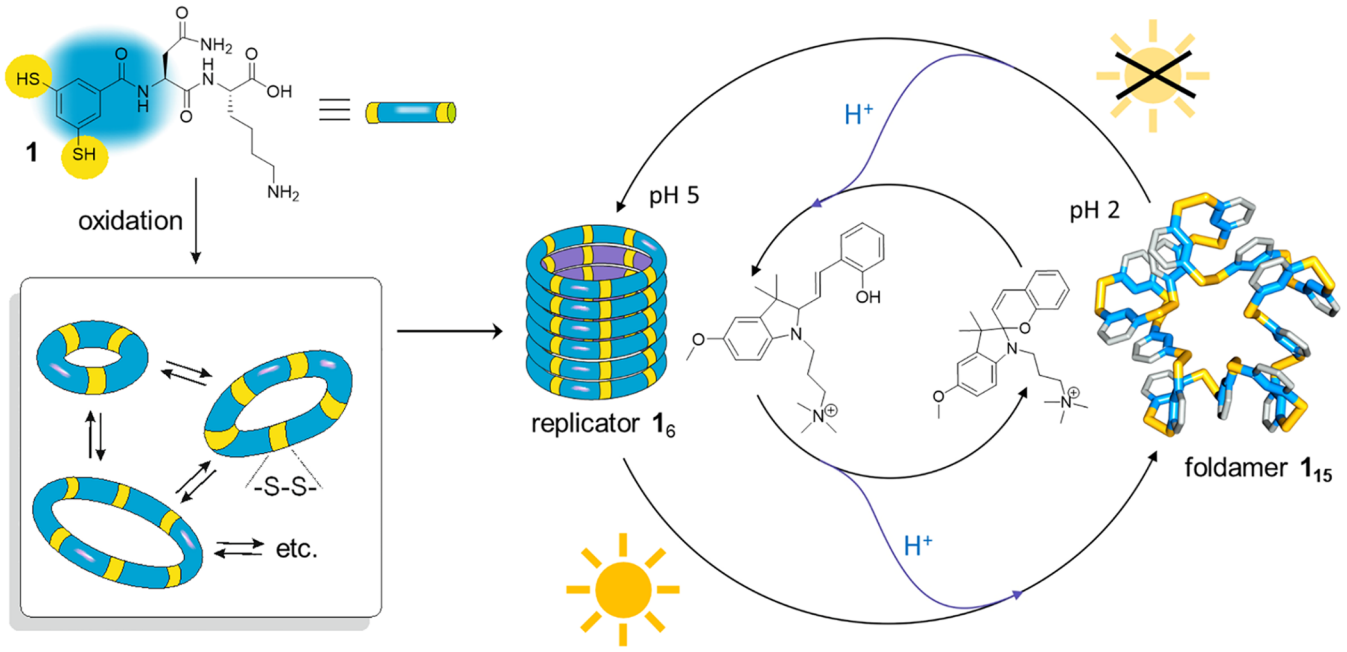

[a]Photoirradiation releases protons from a photoacid that causes the destabilization of fibrous aggregates of 1_6 and its conversion into foldamer 1_{15}. When irradiation is halted, the protons return to the photoacid and the replicator re-forms at the expense of the foldamer.

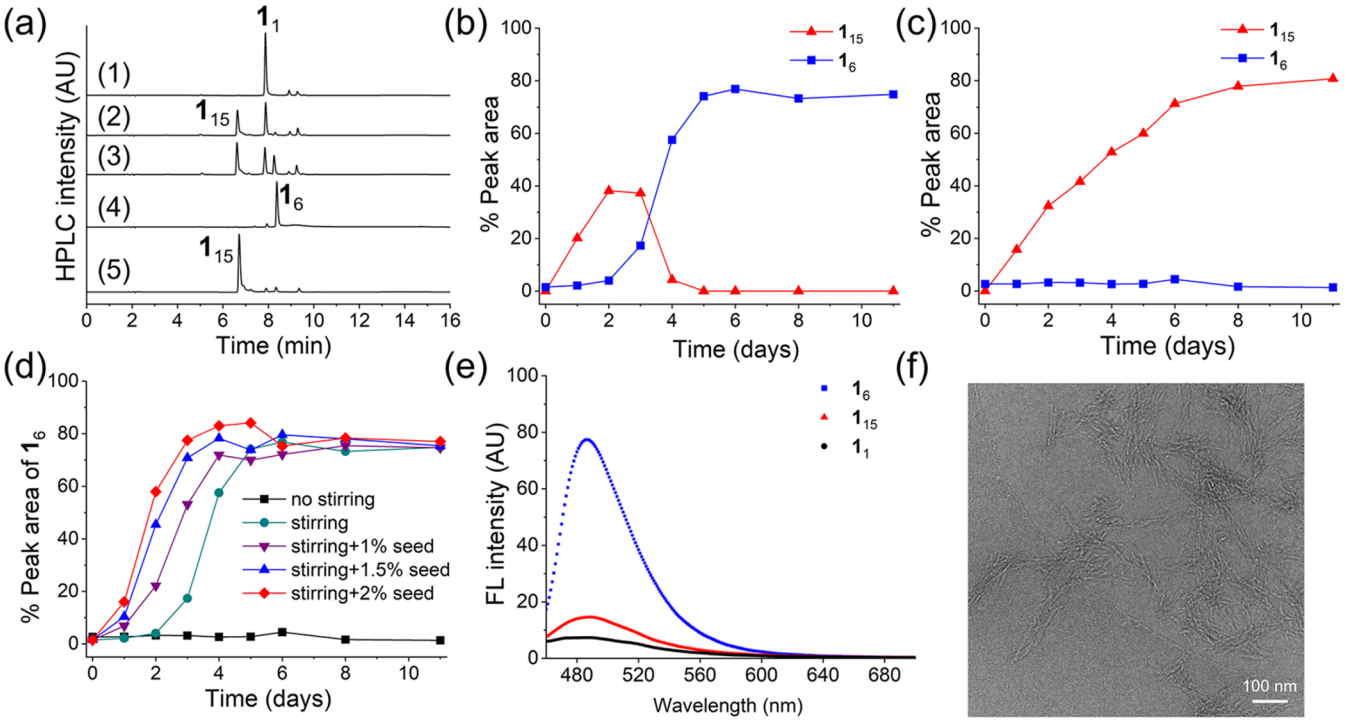

Figure 1. Selective and spontaneous formation of either a self-replicator or a foldamer depending on mechanical agitation. (a) Ultra-high-performance liquid chromatography (UHPLC) of the dynamic combinatorial libraries (DCLs) made from 1.0 mM **1** under magnetic stirring (600 rpm) at day 0 (trace 1), day 2 (trace 2), day 3 (trace 3), and day 8 (trace 4) in 50 mM borate buffer, pH 8.2, 30 °C. Trace 5 shows the UHPLC chromatogram of the DCL without stirring at day 8. (b) Kinetic profiles for libraries prepared from 1.0 mM of building block **1** at 30 °C in 50 mM borate buffer, pH 8.2 under magnetic stirring (600 rpm) and (c) without stirring. (d) Kinetic profiles for libraries prepared from 1.0 mM of building block **1** in 50 mM borate buffer (pH 8.2) with the addition of different amounts of the preformed 1_6 as the seed at day 0. (e) Thioflavin T fluorescence emission spectra of DCLs dominated by 1_6, 1_{15}, or 1_1. (f) Cryo-transmission electron microscopy (Cryo-TEM) image of the 1_6 fibers. Scale bar: 100 nm.

https://doi.org/10.1021/jacs.4c09114
J. Am. Chem. Soc. 2024, 146, 33395−33402

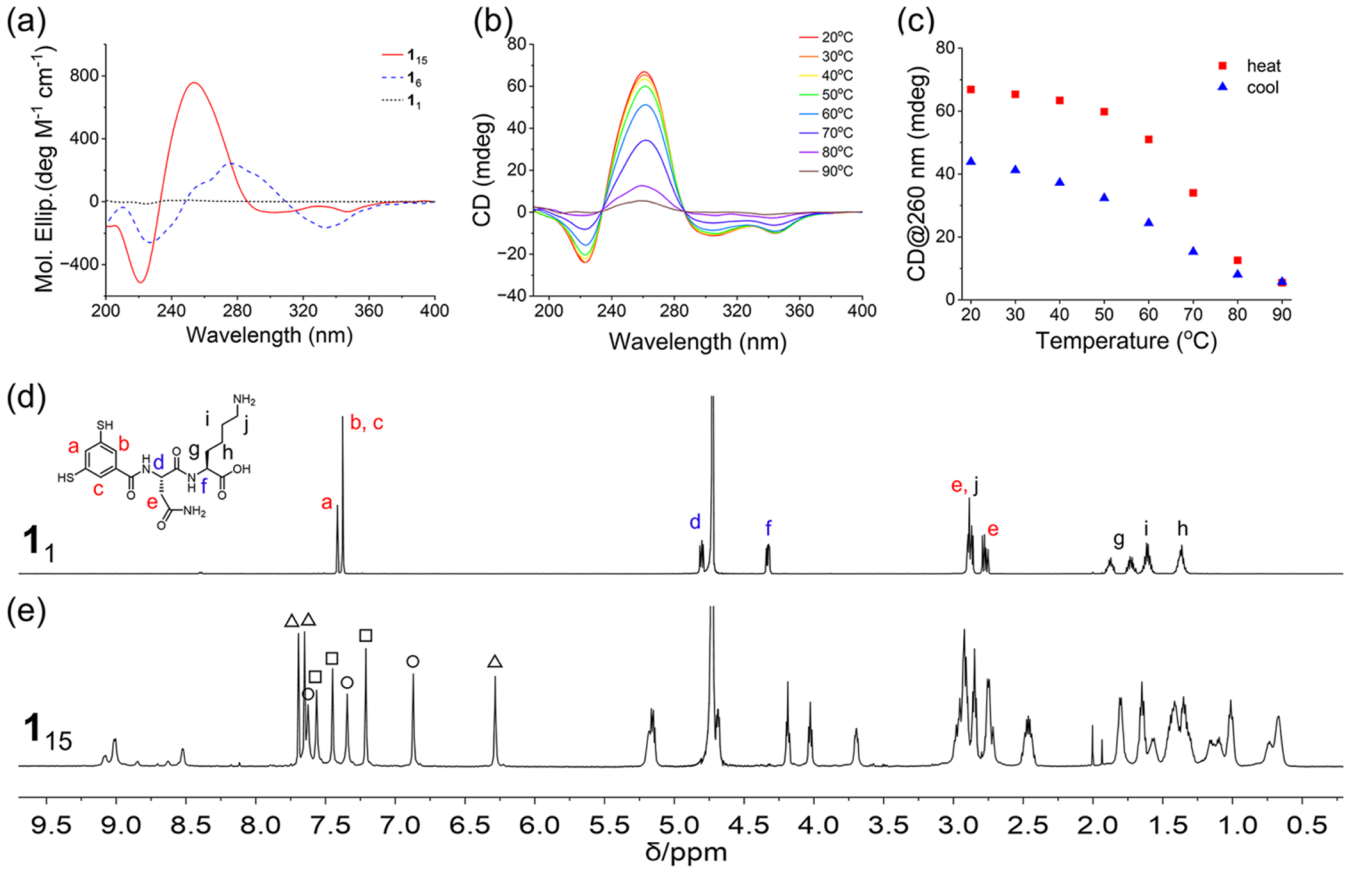

Figure 2. Characterization of $\mathbf{1}_{15}$ by CD and NMR. (a) CD spectra of $\mathbf{1}_{15}$, $\mathbf{1}_6$, and $\mathbf{1}_1$. (b) Variable-temperature CD spectra of $\mathbf{1}_{15}$ from 20 to 90 °C. (c) Changes in ellipticity at 260 nm of $\mathbf{1}_{15}$ upon a heat−cool cycle. ^{1}H NMR spectra of (d) $\mathbf{1}_1$ and (e) $\mathbf{1}_{15}$ in D_2O (600 MHz). The peaks marked with triangles, circles, and squares belong to the aromatic protons of three distinct phenyl rings, respectively (inferred from the total correlation spectroscopy (TOCSY) in Figure S10). The exact assignment to a-, b-, and c-type protons was not performed.

RESULTS AND DISCUSSION

Building Block Design and Mechanoresponsiveness of the Dynamic Combinatorial Library. As part of our exploration of dipeptide-appended dithiol building blocks to access large macrocyclic foldamers,[21,22] we designed building block **1** (Scheme 1). An asparagine residue was introduced to provide directional interactions (hydrogen bonds) that are important to stabilize specific folded structures. A lysine residue at the C-terminus makes the building block zwitterionic at neutral pH, ensuring sufficient water solubility. Oxidation of building block **1** in borate buffer (pH 8.2) under magnetic stirring (600 rpm) led to the rapid formation of macrocycle $\mathbf{1}_{15}$, consisting of 15 subunits of **1** (traces 1 and 2 in Figure 1a,b). In the subsequent days, the concentration of $\mathbf{1}_{15}$ gradually diminished and gave way to hexameric macrocycle $\mathbf{1}_6$, which appears to be the thermodynamic product (Figure 1a(3, 4),b). However, $\mathbf{1}_{15}$ can be obtained selectively and remained stable for a least 1 month, when the same experiment was conducted without agitation (see trace 5 in Figures 1a,c and S2−S7). Seeding experiments were performed to investigate whether the formation of $\mathbf{1}_6$ is an autocatalytic process. As shown in Figure 1d, when a fresh library was seeded with preformed $\mathbf{1}_6$ its rate of formation increased compared to the samples, where no seed was added. The effect was more pronounced when the amount of seed increased from 1 to 2%. These results confirm that $\mathbf{1}_6$ is a self-replicator. The observation that stirring promotes the formation of $\mathbf{1}_6$ is consistent with growth through a fiber elongation−fragmentation mechanism, as proposed previously for similar self-replicating molecules.[35] In the absence of stirring, fibers do not readily fragment, and the growth of $\mathbf{1}_6$ is hampered, allowing $\mathbf{1}_{15}$ to persist. Note that stirring speed influences the rate of replicator formation,[35] but that harsher methods like sonication have been found to degrade the material due to overoxidation of the disulfide linkages to sulfinic and sulfonic acids.

We conducted thioflavin T assays (Figure 1e), which showed enhanced fluorescence at 487 nm in the presence of $\mathbf{1}_6$ but not for $\mathbf{1}_{15}$ and $\mathbf{1}_1$, indicative of β-sheet-like structures in the assemblies of $\mathbf{1}_6$. Cryo-TEM images of a sample dominated by $\mathbf{1}_6$ showed bundles of fibers that, individually, have a diameter of 3.5 nm (Figure 1f). This dimension is in agreement with the diameter of a single hexamer macrocycle, with peptide chains extending radially from the dimercaptobenzene core.

Characterization of the 15mer Foldamer. Macrocycle $\mathbf{1}_{15}$ was purified by HPLC and characterized with circular dichroism (CD), ^{1}H NMR spectroscopy, and X-ray crystallography. While the solution of building block **1** showed only weak CD signals, $\mathbf{1}_{15}$ gave an intense positive band at 260 nm, indicating that the aromatic core experiences a chiral environment (Figure 2a). In comparison, $\mathbf{1}_6$ shows a positive peak at 278 nm. The bathochromic shift of the band with respect to $\mathbf{1}_{15}$ was assigned to π-stacked phenyl rings. A shoulder at 260 nm was also detected. In addition, the maximum at around 210 nm and the minimum at around 230

https://doi.org/10.1021/jacs.4c09114
J. Am. Chem. Soc. 2024, 146, 33395−33402

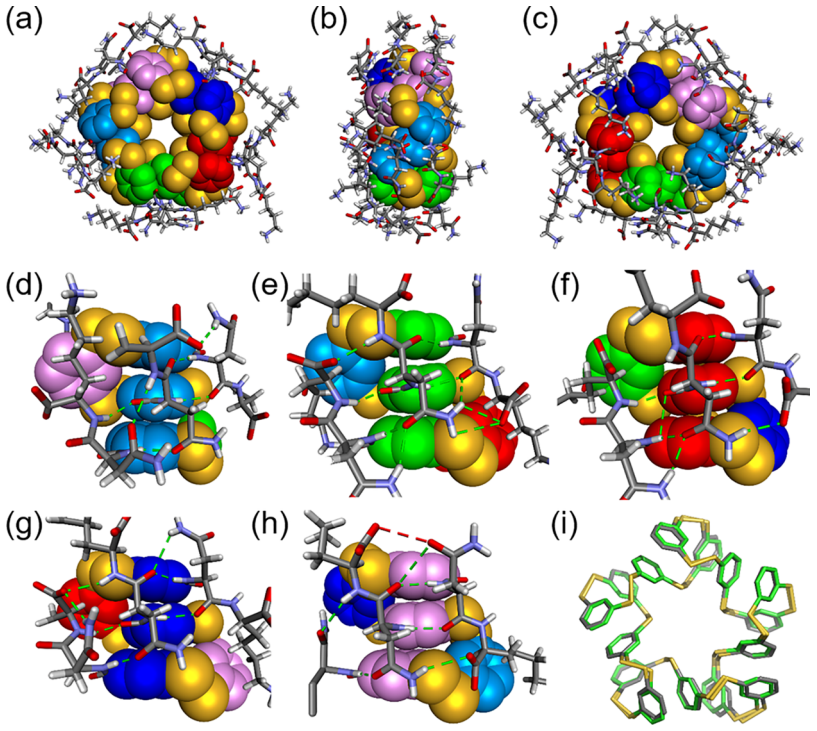

Figure 3. Crystal structure of foldamer $\mathbf{1}_{15}$. (a) Top, (b) side, and (c) bottom views of the color-coded space-filling representation of the hydrophobic dimercaptobenzene core and tube representation of the side chains of L-$\mathbf{1}_{15}$ from the crystal structure of L/D-$\mathbf{1}_{15}$. (d–h) Front view of the five stacks of the three core benzene rings, highlighting the arrays of hydrogen bonds (green dashes), (h) also highlighting the $-CO_2H\cdots O{=}C$ contact (red dashes). (i) Tube representation of the hydrophobic core of L-$\mathbf{1}_{15}$ (gray) aligned sterically to the hydrophobic core of an analogous pentagonal structure (green) formed from the assembly of 15 units of building block bearing aspartic acid and an adenine residue instead of the dipeptide in **1**.[21]

nm suggest the formation of *β*-sheet structures in the assemblies of $\mathbf{1}_6$. Temperature-dependent CD experiments show that the signal of $\mathbf{1}_{15}$ at 260 nm decreases by 92% after the temperature is increased from 20 to 90 °C (Figure 2b). The signal recovered only 66% of its original value when the temperature was decreased back to 20 °C (Figures 2c and S8a). HPLC analysis of the sample showed that $\mathbf{1}_{15}$ had decomposed to smaller macrocycles after the heat–cool cycle (Figure S8b). For the $\mathbf{1}_6$ sample (Figure S9a), the CD signal at 278 nm decreased by 53% after elevating the temperature from 20 to 90 °C but recovered 84% after cooling. HPLC analysis of the sample indicated that $\mathbf{1}_6$ was partially converted to larger macrocycles upon thermal cycling (Figure S9b).

The solution-phase ^{1}H NMR spectra (D_2O, 298 K) of $\mathbf{1}_1$ and $\mathbf{1}_{15}$ are shown in Figure 2d,e. Foldamer $\mathbf{1}_{15}$ shows three sets of signals for the aromatic protons (from 6.3 to 7.8 ppm), which suggests that $\mathbf{1}_{15}$ has an average C_5 symmetry. Furthermore, the pairs of aromatic protons *ortho* to each benzamide function (labeled b and c in Figure 2d) appear as distinct signals in the spectrum of $\mathbf{1}_{15}$, indicating a loss of symmetry for each building block (also see TOCSY spectrum in Figure S10). The large upfield chemical shifts of two phenyl protons to 6.9 and 6.3 ppm indicate that some of these protons are adjacent to the face of an aromatic ring. The sharp and well-defined NMR spectrum suggests that $\mathbf{1}_{15}$ adopts a highly ordered structure in solution.

The crystal structure of $\mathbf{1}_{15}$ shows that the 15 dimercaptobenzene moieties collapse into a dense hydrophobic core exposing their hydrophilic appendages at the surface, resembling the folding of proteins (Figures 3, S12, and S13). The structure is very well-defined with 14 out of 15 lysine residues being visible in the electron-density map. Five identical stacks of three phenyl rings are found in the core, consistent with the 5-fold symmetry observed in the NMR spectrum. Overlay of this core structure with another previously discovered 15mer fold[21] indicates that they are very similar (Figure 3i). The similarity in the folding of the hydrophobic core is remarkable, given that the previously reported 15mer is made from a building block that has a substantially different structure, featuring an aspartic acid and an adenine residue instead of the dipeptide of **1**. Most of the butyl chains of the lysine residues of $\mathbf{1}_{15}$ lay down on the aromatic core and establish hydrophobic contacts with the faces of the stacks of the three benzene rings. In the previously described 15mer, adenine rings were found to stack at these positions. Extensive hydrogen bonding occurs between dipeptide residues within each of the five subsets of $\mathbf{1}_{15}$ but not between them (Figure 3d–h). Apart from the amide bonds in the peptide backbone, the side-chain amides from asparagine together with side-chain amines and C-terminal carboxylate groups from lysine are shown to play an important role in these hydrogen-bonding interactions. Note that the hydrogen-bonding patterns differ from subset to subset in the crystal structure (Figure 3d–h). These different patterns must exchange rapidly on the NMR time scale to give rise to the observed average 5-fold symmetry.

Foldamer $\mathbf{1}_{15}$ and Replicator $\mathbf{1}_6$ Interconvert upon Changing the pH. Further investigation revealed that lowering the pH favors the formation of the 15mer foldamer and inhibits the formation of the competing replicator, even under magnetic stirring. As shown in Figures 4a and S14, when the pH was high (i.e., pH 8.2, 7.3, 6.4, and 5.3), replicator $\mathbf{1}_6$

https://doi.org/10.1021/jacs.4c09114
J. Am. Chem. Soc. 2024, 146, 33395–33402

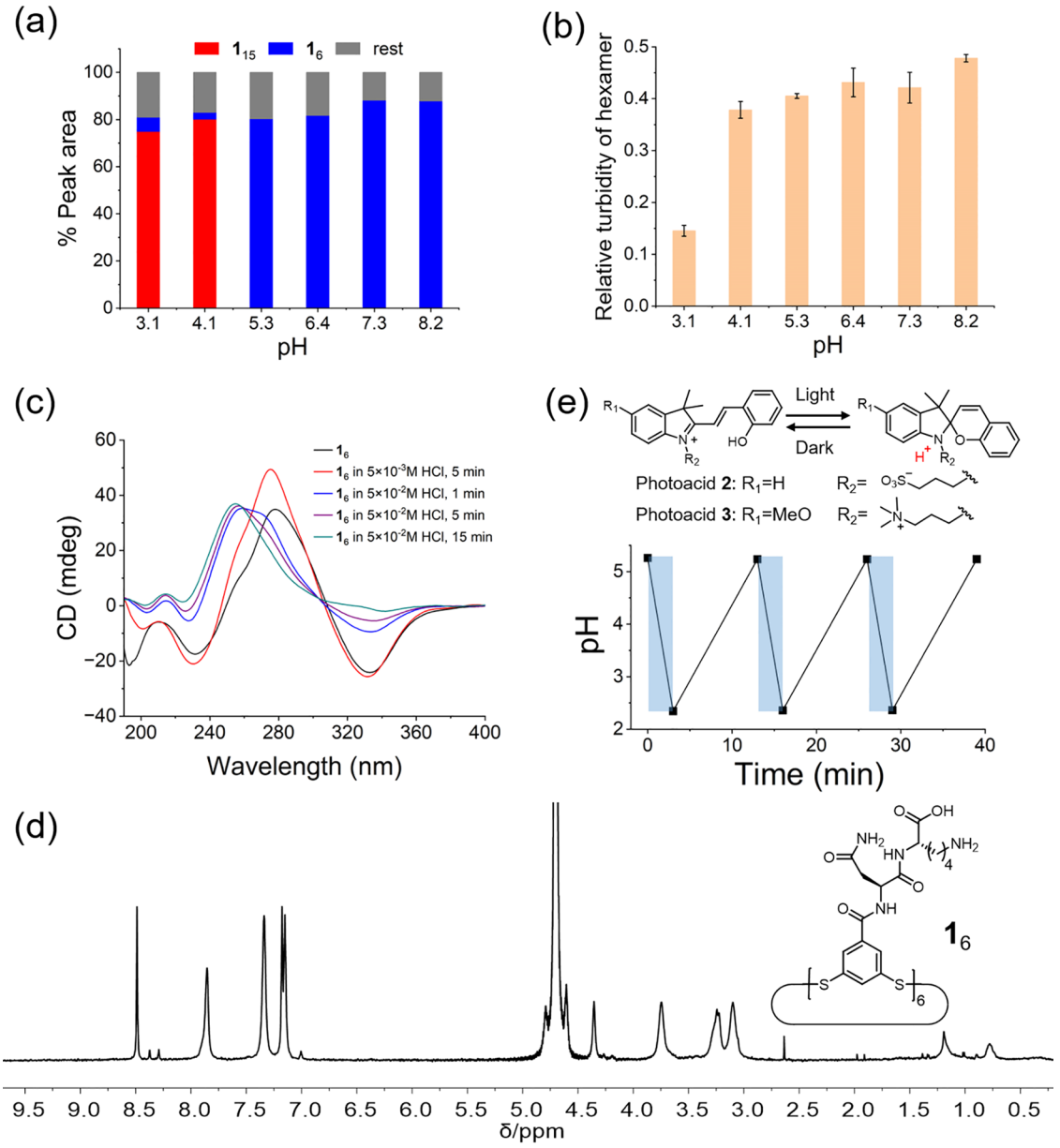

Figure 4. Effect of pH on the formation of foldamer $\mathbf{1}_{15}$ and replicator $\mathbf{1}_6$. (a) UHPLC peak area ratios for libraries prepared from 1.0 mM building block **1** in citrate-phosphate buffer of different pH values after 8 days of magnetic stirring (600 rpm). (b) Relative turbidity of a sample of preformed fibers of $\mathbf{1}_6$ (0.40 mM in building block **1**) in citrate-phosphate buffer solutions of different pH values. Relative turbidity was calculated as $(A - A_0)/A_0$, where A is the absorbance of $\mathbf{1}_6$ sample at 650 nm, and A_0 is the absorbance of the corresponding buffer at 650 nm. (c) CD spectra of $\mathbf{1}_6$ in water after adding different amounts of HCl. (d) ^{1}H NMR spectrum of $\mathbf{1}_6$ in D_2O containing 0.5 M HCl (600 MHz). (e) Chemical structures of two photoacids and the pH change of a photoacid **3** (MCH) solution upon alternating between periods of irradiation and no irradiation. For each cycle, a solution of MCH at a concentration of 5.0 mM was irradiated with an light-emitting diode (LED) (450 nm) for 3 min and kept in the dark for 10 min. Blue shading indicates the periods of irradiation.

dominated the library, while at lower pH (i.e., pH 4.1 and 3.1), $\mathbf{1}_{15}$ was formed selectively. Some rationale for the stability of $\mathbf{1}_{15}$ at low pH was found in its crystal structure (Figure 3h).

The crystallization of $\mathbf{1}_{15}$ was performed at a pH above 8.0. C-terminal functions thus exist as carboxylates. Only two of them were found to be involved in "salt-bridges", i.e., charge-reinforced hydrogen bonds, with lysine residues ($d_{N\cdots O}$ < 3.5 Å) susceptible to be altered upon protonation of the carboxylate. The others are either simply exposed to the water (five) or hydrogen-bonded to peptidic or Asn amide protons, that is, less susceptible to alter the overall fold stability upon carboxylate protonation. In some cases, carboxylate protonation may even provide an additional hydrogen bond involving the acid proton as a donor.

In contrast, even though the structure of replicator $\mathbf{1}_6$ is unknown, its assembly is hampered upon acidifying the medium: both the assembly of $\mathbf{1}_6$ into fibers and associations between these fibers are disrupted. Evidence comes from UV−vis, CD, TEM, and NMR data. The aggregation of preformed $\mathbf{1}_6$ fibers in buffer solutions of different pH values was analyzed by UV−vis spectroscopy and turbidity measurement (absorbance at 650 nm; Figure 4b). As the pH of the solution was changed from high (8.2, 7.3, 6.4, 5.3, 4.1) to low (3.1); the turbidity of the $\mathbf{1}_6$ sample decreased significantly, indicating

https://doi.org/10.1021/jacs.4c09114
J. Am. Chem. Soc. 2024, 146, 33395−33402

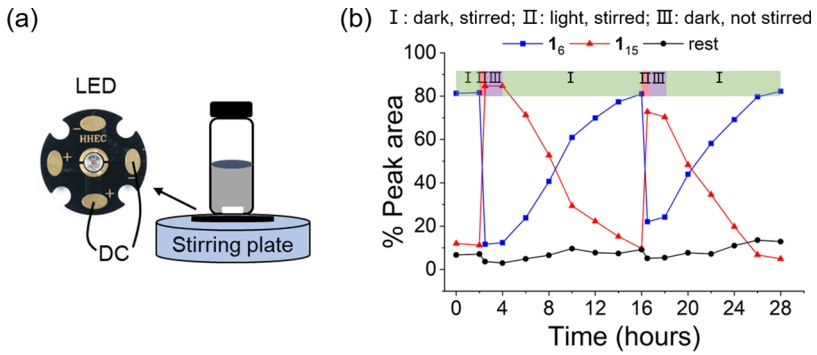

Figure 5. Light-controlled interconversion between the replicator and foldamer. (a) Experimental setup in which a DCL in the presence of photoacid **3** was irradiated by an LED and magnetically stirred at 600 rpm. A nitrogen atmosphere was used to prevent the rapid oxidation of free thiols in the sample. (b) Kinetic profile of the dynamic library made from **1** in the presence of photoacid **3** (5.0 mM) during two light irradiation−darkness cycles. The experiment was started from premade fibers of $\mathbf{1}_6$ to which 0.10 equiv of **1** was added to mediate disulfide exchange. The initial pH of the solution was 5.2.

that the $\mathbf{1}_6$ fibers are less aggregated at lower pH. The effect of pH on the assembly of $\mathbf{1}_6$ was investigated by CD and TEM. As shown in Figure 4c, when different amounts of HCl were added to a sample of $\mathbf{1}_6$ fibers, the peak intensity at 278 and 330 nm, which are characteristic for fibers of stacks of $\mathbf{1}_6$, first increased a little but then gradually diminished, with the emergence of a new peak at around 260 nm. HPLC analysis (Figure S15b) showed that the $\mathbf{1}_6$ rings nevertheless remained intact, suggesting that the shift of the CD signal can be attributed to a change in the mode of assembly of $\mathbf{1}_6$. Variable-temperature CD data of a sample of $\mathbf{1}_6$ in the presence of 50 mM HCl (Figure S15a) exhibit a decrease and complete recovery of the CD signal at 260 nm during a heat−cool cycle (20−80−20 °C). HPLC analysis of the same sample confirmed that $\mathbf{1}_6$ remained intact during this treatment (Figure S15b). Negative stain TEM images showed that at lower pH, fibers disassembled into smaller ones (Figure S16). Finally, ^{1}H NMR spectra of a sample of $\mathbf{1}_6$ in the presence of 0.5 M HCl (Figure 4d) exhibited sharp peaks, which indicated the presence of unstacked hexamer rings. In contrast, no signals were detected in NMR spectra of samples of fibrous $\mathbf{1}_6$ at close-to-neutral pH. Different from ^{1}H NMR spectra of building blocks **1** and $\mathbf{1}_{15}$ (Figure 2d,e), downfield-shifted signals (i.e., 8.49 and 7.86 ppm) were detected for $\mathbf{1}_6$ (Figure 4d). HPLC analysis confirmed that $\mathbf{1}_6$ in a 0.5 M HCl solution remained stable for 11 days (Figure S17).

We speculate that when the pH is lower than the pK_a of carboxylic acid (typically in the range of 4.2−4.7), building block **1** will attain a net positive charge, resulting in electrostatic repulsion that will destabilize the fibers of $\mathbf{1}_6$. When there is sufficient thiol available for disulfide exchange, such destabilization will then result in a re-equilibration in favor of foldamer $\mathbf{1}_{15}$.

Light-Controlled Interconversion between Replicator and Foldamer. The pH responsiveness of the system provides an opportunity for the dynamic switching between the 15mer foldamer and hexamer self-replicator. At higher pH, the thermodynamically more stable hexamer fiber dominates the library at the expense of the other species. At lower pH, hexamer fibers disassemble and the formation of the 15mer foldamer becomes favored. We reasoned that it should be possible to drive the interconversion between the two oligomers by the photoirradiation of an appropriately chosen photoacid. We first tested photoacid **2** (Figure 4e).[36] However, the poor hydrolytic stability[37] of this compound, together with its limited solubility, restricted its use. We then focused on the recently developed photoacid **3**[38,39] (Figure 4e). This compound has a methoxy group on the indolinium ring, which was reported to improve hydrolytic stability. Furthermore, its positively charged alkyl ammonium side chain greatly enhances its water solubility, which enables a wider pH switching window. Upon light irradiation, the open-ring protonated merocyanine (MCH) switches to the closed spiropyran form (SP) with the release of a proton. As shown in Figure S19, the UV-vis spectrum of MCH before irradiation exhibited a characteristic adsorption peak at 440 nm, which decreased upon 10 s of irradiation, while the peak at 242 nm increased, which was attributed to the spiropyran form. The pH of the MCH aqueous solution (5.0 mM) changed from 5.2 to 2.4 upon irradiation. When irradiation is stopped, the absorbance at 440 nm restores in 5 min and the pH returns to the original value (Figure 4e). Such a pH switching range fits well with the pH change needed for interconverting replicator and foldamer.

We then probed the photomediated interconversion between these two compounds using the setup shown in Figure 5a. Reaction monitoring was performed by UHPLC. The strong absorbance of photoacid **3** did not allow for simultaneous monitoring by CD because the transmittance was too low. We started from a mixture of $\mathbf{1}_6$ fibers and MCH that was stable as long as it was not irradiated (Figures 5b and S20). When the light was switched on (at t = 2 h) for 30 min, the concentration of foldamer $\mathbf{1}_{15}$ increased rapidly and dominated the library, while replicator $\mathbf{1}_6$ was consumed. We then turned off the light and the stirring, whereafter the composition of the library barely changed, as the system became trapped in a metastable state (from 2.5 to 4 h). When stirring was commenced, $\mathbf{1}_6$ grew to dominate the library in the course of 12 h. A second round of switching between replicators and foldamers was also realized by another light−dark cycle. Thus, through the use of light as a source of energy, the system can be taken out of its equilibrium state, where it is dominated by replicator $\mathbf{1}_6$ and form a dissipative stationary state dominated by foldamer $\mathbf{1}_{15}$ that could be maintained as long as it was irradiated (Scheme 1).

CONCLUSIONS

We have demonstrated the spontaneous formation of a foldamer, consisting of 15 building block units, or a self-

https://doi.org/10.1021/jacs.4c09114
J. Am. Chem. Soc. 2024, 146, 33395−33402

replicator, consisting of 6 building block units, from a dynamic combinatorial library upon oligomerization of building block **1**, as well as their interconversion triggered by a change in agitation regime or pH.

In general, in dynamic combinatorial libraries, smaller compounds, like dimers, trimers, and tetramers, tend to be the thermodynamically more stable species, as producing a large number of small library members is entropically favorable over producing a smaller number of larger library members. However, the formation of noncovalent interactions (enthalpy-driven, if we disregard (de)solvation effects) by specific library members can overcome this inherent bias. In the present systems, at moderately elevated pH, these noncovalent interactions form either intermolecularly (driving the self-assembly of $\mathbf{1}_6$ into a supramolecular polymer) or intramolecularly (driving the folding of $\mathbf{1}_{15}$). At this pH, the nucleation of the fiber is accompanied by a large kinetic barrier (most likely the result of the large entropic penalty associated with the conformational rearrangement of the interacting molecules), while, perhaps counterintuitively, the foldamer forms more readily. So, the pathway to foldamer formation is associated with a lower kinetic barrier than that leading to replicator nucleation. However, once an autocatalytic path (promoted by fiber fragmentation upon agitation) opens up, it outcompetes foldamer formation and even converts the already formed foldamers into thermodynamically more stable replicators.

Mechanical agitation at close-to-neutral pH enables the conversion of foldamer $\mathbf{1}_{15}$ to thermodynamically more stable self-replicator $\mathbf{1}_6$, while lowering the pH causes foldamer $\mathbf{1}_{15}$ to become the dominant species. Using a photoacid, the interconversion between the replicator and foldamer was achieved by switching photoirradiation on or off. Here, the energy of light was used to move the system away from the equilibrium state, where the replicator dominates, to produce a high steady-state concentration of foldamer that was maintained as long as irradiation continued. This light-mediated switching between replicator and foldamer states complements other work, published in this issue, in which homeostatically populating the foldamer state was based on chemical fueling, requiring the continuous supply of building block material. Coupling between replication and foldamer formation creates a system where both species can be accessed and constitutes a primitive way of coupling a genotype (the replicator) to a phenotype (the foldamer). The challenge is now to endow the foldamer with a function (for example, catalytic activity) that would benefit the system, which would allow for the selection of such genotype−phenotype coupling in the course of the Darwinian evolution.

■ ASSOCIATED CONTENT

Supporting Information

The Supporting Information is available free of charge at https://pubs.acs.org/doi/10.1021/jacs.4c09114.

General procedures, building block synthesis, library preparation, UHPLC-MS analysis, thioflavin T fluorescence, (cryo-)TEM, (variable temperature) circular dichroism, turbidity, NMR and X-ray crystallography data, pH measurements, and light-triggered switching between self-replicator and foldamers (PDF)

Accession Codes

Deposition Number 2209327 contains the supplementary crystallographic data for this paper. These data can be obtained free of charge via the joint Cambridge Crystallographic Data Centre (CCDC) and Fachinformationszentrum Karlsruhe Access Structures service.

■ AUTHOR INFORMATION

Corresponding Authors

Yulong Jin − *Beijing National Laboratory for Molecular Sciences, CAS Key Laboratory of Analytical Chemistry for Living Biosystems, Institute of Chemistry, Chinese Academy of Sciences, 100190 Beijing, China; State Key Laboratory of Chemical Resource Engineering, Beijing Advanced Innovation Center for Soft Matter Science and Engineering, College of Chemistry, Beijing University of Chemical Technology, 100029 Beijing, China;* orcid.org/0000-0003-1359-3274; Email: jinyulong@buct.edu.cn

Ivan Huc − *Department of Pharmacy, Ludwig-Maximilians-Universität München, 81377 Munich, Germany;* orcid.org/0000-0001-7036-9696; Email: ivan.huc@cup.lmu.de

Sijbren Otto − *Centre for Systems Chemistry, Stratingh Institute, University of Groningen, 9747 AG Groningen, The Netherlands;* orcid.org/0000-0003-0259-5637; Email: s.otto@rug.nl

Authors

Pradeep K. Mandal − *Department of Pharmacy, Ludwig-Maximilians-Universität München, 81377 Munich, Germany;* orcid.org/0000-0001-5996-956X

Juntian Wu − *Centre for Systems Chemistry, Stratingh Institute, University of Groningen, 9747 AG Groningen, The Netherlands;* orcid.org/0000-0003-3894-9812

Armin Kiani − *Centre for Systems Chemistry, Stratingh Institute, University of Groningen, 9747 AG Groningen, The Netherlands*

Rui Zhao − *Beijing National Laboratory for Molecular Sciences, CAS Key Laboratory of Analytical Chemistry for Living Biosystems, Institute of Chemistry, Chinese Academy of Sciences, 100190 Beijing, China;* orcid.org/0000-0001-7191-9354

Complete contact information is available at: https://pubs.acs.org/10.1021/jacs.4c09114

Notes

The authors declare no competing financial interest.

■ ACKNOWLEDGMENTS

The authors thank Marc Geerts, Dr. Meagan Beatty, Ankush Sood, and Dr. Kai Liu for useful discussions and Dr. L. McGregor (ID23-2, ESRF) for assistance during data collection at the synchrotron beamline. The authors are grateful to the financial support from the Dutch Ministry of Education, Culture and Science (Gravitation program 024.001.035), the China Scholarship Council, the Fundamental Research Funds for the Central Universities (buctrc202415), the Beijing Natural Science Foundation (2242027), the National Natural Science Foundation of China (22174145), and the Deutsche Forschungsgemeinschaft (Project #HU 1766/5-1 to I.H.).

REFERENCES

(1) Otto, S. An Approach to the De Novo Synthesis of Life. *Acc. Chem. Res.* **2022**, *55*, 145−155.
(2) Ruiz-Mirazo, K.; Briones, C.; de la Escosura, A. Prebiotic Systems Chemistry: New Perspectives for the Origins of Life. *Chem. Rev.* **2014**, *114*, 285−366.
(3) Müller, F.; Escobar, L.; Xu, F.; Wegrzyn, E.; Nainyte, M.; Amatov, T.; Chan, C. Y.; Pichler, A.; Carell, T. A prebiotically plausible scenario of an RNA-peptide world. *Nature* **2022**, *605*, 279−284.
(4) Patzke, V.; von Kiedrowski, G. Self replicating systems. *Arkivoc* **2007**, *v*, 293−310.
(5) Paul, N.; Joyce, G. F. A self-replicating ligase ribozyme. *Proc. Natl. Acad. Sci. U.S.A.* **2002**, *99*, 12733−12740.
(6) Draper, W. E.; Hayden, E. J.; Lehman, N. Mechanisms of covalent self-assembly of the Azoarcus ribozyme from four fragment oligonucleotides. *Nucleic Acids Res.* **2007**, *36*, 520−531.
(7) Lee, D. H.; Granja, J. R.; Martinez, J. A.; Severin, K.; Ghadiri, M. R. A self-replicating peptide. *Nature* **1996**, *382*, 525−528.
(8) Yao, S.; Ghosh, I.; Zutshi, R.; Chmielewski, J. Selective amplification by auto- and cross-catalysis in a replicating peptide system. *Nature* **1998**, *396*, 447−450.
(9) Kosikova, T.; Philp, D. Exploring the emergence of complexity using synthetic replicators. *Chem. Soc. Rev.* **2017**, *46*, 7274−7305.
(10) Le Vay, K.; Weise, L. I.; Libicher, K.; Mascarenhas, J.; Mutschler, H. Templated Self-Replication in Biomimetic Systems. *Adv. Biosyst.* **2019**, *3*, No. 1800313.
(11) Hill, D. J.; Mio, M. J.; Prince, R. B.; Hughes, T. S.; Moore, J. S. A field guide to foldamers. *Chem. Rev.* **2001**, *101*, 3893−4011.
(12) Scott Lokey, R.; Iverson, B. L. Synthetic Molecules That Fold into a Pleated Secondary Structure in Solution. *Nature* **1995**, *375*, 303−305.
(13) Appella, D. H.; Christianson, L. A.; Klein, D. A.; Powell, D. R.; Huang, X. L.; Barchi, J. J.; Gellman, S. H. Residue-based control of helix shape in beta-peptide oligomers. *Nature* **1997**, *387*, 381−384.
(14) Goodman, C. M.; Choi, S.; Shandler, S.; DeGrado, W. F. Foldamers as versatile frameworks for the design and evolution of function. *Nat. Chem. Biol.* **2007**, *3*, 252−262.
(15) Guichard, G.; Huc, I. Synthetic foldamers. *Chem. Commun.* **2011**, *47*, 5933−5941.
(16) Chandramouli, N.; Ferrand, Y.; Lautrette, G.; Kauffmann, B.; Mackereth, C. D.; Laguerre, M.; Dubreuil, D.; Huc, I. Iterative design of a helically folded aromatic oligoamide sequence for the selective encapsulation of fructose. *Nat. Chem.* **2015**, *7*, 334−341.
(17) Le Bailly, B. A. F.; Clayden, J. Dynamic foldamer chemistry. *Chem. Commun.* **2016**, *52*, 4852−4863.
(18) Girvin, Z. C.; Andrews, M. K.; Liu, X. Y.; Gellman, S. H. Foldamer-templated catalysis of macrocycle formation. *Science* **2019**, *366*, 1528−1531.
(19) Martinek, T. A.; Fülöp, F. Peptidic foldamers: ramping up diversity. *Chem. Soc. Rev.* **2012**, *41*, 687−702.
(20) Ashkenasy, G.; Hermans, T. M.; Otto, S.; Taylor, A. F. Systems chemistry. *Chem. Soc. Rev.* **2017**, *46*, 2543−2554.
(21) Liu, B.; Pappas, C. G.; Zangrando, E.; Demitri, N.; Chmielewski, P. J.; Otto, S. Complex molecules that fold like proteins can emerge spontaneously. *J. Am. Chem. Soc.* **2019**, *141*, 1685−1689.
(22) Pappas, C. G.; Mandal, P. K.; Liu, B.; Kauffmann, B.; Miao, X.; Komáromy, D.; Hoffmann, W.; Manz, C.; Chang, R.; Liu, K.; Pagel, K.; Huc, I.; Otto, S. Emergence of low-symmetry foldamers from single monomers. *Nat. Chem.* **2020**, *12*, 1180−1186.
(23) Carnall, J. M. A.; Waudby, C. A.; Belenguer, A. M.; Stuart, M. C. A.; Peyralans, J. J. P.; Otto, S. Mechanosensitive Self-Replication Driven by Self-Organization. *Science* **2010**, *327*, 1502−1506.
(24) Monreal Santiago, G.; Liu, K.; Browne, W. R.; Otto, S. Emergence of light-driven protometabolism on recruitment of a photocatalytic cofactor by a self-replicator. *Nat. Chem.* **2020**, *12*, 603−607.
(25) Pappas, C. G.; Liu, B.; Maric, I.; Ottele, J.; Kiani, A.; van der Klok, M. L.; Onck, P. R.; Otto, S. Two Sides of the Same Coin: Emergence of Foldamers and Self-Replicators from Dynamic Combinatorial Libraries. *J. Am. Chem. Soc.* **2021**, *143*, 7388−7393.
(26) Liu, B.; Beatty, M. A.; Pappas, C. G.; Liu, K.; Ottele, J.; Otto, S. Self-Sorting in Dynamic Combinatorial Libraries Leads to the Co-Existence of Foldamers and Self-Replicators. *Angew. Chem., Int. Ed.* **2021**, *60*, 13569−13573.
(27) Borsley, S.; Leigh, D. A.; Roberts, B. M. W. Chemical fuels for molecular machinery. *Nat. Chem.* **2022**, *14*, 728−738.
(28) Howlett, M. G.; Engwerda, A. H. J.; Scanes, R. J. H.; Fletcher, S. P. An autonomously oscillating supramolecular self-replicator. *Nat. Chem.* **2022**, *14*, 805−810.
(29) Mattia, E.; Otto, S. Supramolecular systems chemistry. *Nat. Nanotechnol.* **2015**, *10*, 111−119.
(30) Boekhoven, J.; Hendriksen, W. E.; Koper, G. J. M.; Eelkema, R.; van Esch, J. H. Transient assembly of active materials fueled by a chemical reaction. *Science* **2015**, *349*, 1075−1079.
(31) Das, K.; Gabrielli, L.; Prins, L. J. Chemically Fueled Self-Assembly in Biology and Chemistry. *Angew. Chem., Int. Ed.* **2021**, *60*, 20120−20143.
(32) Selmani, S.; Schwartz, E.; Mulvey, J. T.; Wei, H.; Grosvirt-Dramen, A.; Gibson, W.; Hochbaum, A. I.; Patterson, J. P.; Ragan, R.; Guan, Z. Electrically Fueled Active Supramolecular Materials. *J. Am. Chem. Soc.* **2022**, *144*, 7844−7851.
(33) Rizzuto, F. J.; Platnich, C. M.; Luo, X.; Shen, Y.; Dore, M. D.; Lachance-Brais, C.; Guarne, A.; Cosa, G.; Sleiman, H. F. A dissipative pathway for the structural evolution of DNA fibres. *Nat. Chem.* **2021**, *13*, 843−849.
(34) Kundu, P. K.; Samanta, D.; Leizrowice, R.; Margulis, B.; Zhao, H.; Borner, M.; Udayabhaskararao, T.; Manna, D.; Klajn, R. Light-controlled self-assembly of non-photoresponsive nanoparticles. *Nat. Chem.* **2015**, *7*, 646−652.
(35) Colomb-Delsuc, M.; Mattia, E.; Sadownik, J. W.; Otto, S. Exponential self-replication enabled through a fibre elongation/breakage mechanism. *Nat. Commun.* **2015**, *6*, No. 7427.
(36) Shi, Z.; Peng, P.; Strohecker, D.; Liao, Y. Long-lived photoacid based upon a photochromic reaction. *J. Am. Chem. Soc.* **2011**, *133*, 14699−703.
(37) Abeyrathna, N.; Liao, Y. Stability of merocyanine-type photoacids in aqueous solutions. *J. Phys. Org. Chem.* **2017**, *30*, No. e3664.
(38) Wimberger, L.; Prasad, S. K. K.; Peeks, M. D.; Andreasson, J.; Schmidt, T. W.; Beves, J. E. Large, tunable, and reversible pH changes by merocyanine photoacids. *J. Am. Chem. Soc.* **2021**, *143*, 20758−20768.
(39) Berton, C.; Busiello, D. M.; Zamuner, S.; Scopelliti, R.; Fadaei-Tirani, F.; Severin, K.; Pezzato, C. Light-Switchable Buffers. *Angew. Chem., Int. Ed.* **2021**, *60*, 21737−21740.

https://doi.org/10.1021/jacs.4c09114
J. Am. Chem. Soc. 2024, 146, 33395−33402